

# Infinite Dilution Diffusion Coefficients: Benzene Derivatives as Solutes in Supercritical Carbon Dioxide

Julio L. Bueno,\* Juan J. Suárez, Julián Dizy, and Ignacio Medina

Department of Chemical Engineering, University of Oviedo, 33071 Oviedo, Spain

Binary diffusion coefficients of benzene, toluene, ethylbenzene, *n*-propylbenzene, isopropylbenzene, *o*-xylene, *m*-xylene, *p*-xylene, cumene, and mesitylene in CO<sub>2</sub> as a supercritical solvent were determined using the Taylor-Aris dispersion technique. The supercritical fluid phase linear velocity dependence was confirmed in all systems, and the tendency of the dependence of the diffusivity on the molecular size and shape is quantitatively discussed. The influence of pressure and temperature for benzene was extensively studied.

## Introduction

Diffusion coefficients, as well as viscosities and thermal conductivities, are thermophysical properties that describe physical kinetics in transport phenomena, being involved in all the deterministic modelization developed at the microscopic level of description for mass, momentum, and heat transfer, and in heterogeneous chemical kinetics. Thus, diffusion coefficient data are needed in the design of equipment for mass transfer and heterogeneous reaction operations.

Most real situations in these chemical processes, e.g., supercritical extraction, deal with multicomponent mixtures at extreme conditions of temperature and pressure. In contrast, the most consistent theories on the formulation of the diffusion coefficient have arisen from the concept of the mutual diffusion of two components of an isothermal binary mixture in the dilute gas region, either assuming an atomic-molecular theory (a molecule will move as a consequence of a difference in its relative population) or considering the irreversible thermodynamics (there exists a net flux of a given component due to a gradient of its chemical potential).

However, the efforts to determine binary diffusion coefficients are fully justified nowadays. The reasons may be divided into two groups: First, all the forms of mass transfer coefficients, including the most complicated definitions of multicomponent diffusion coefficients, may be assumed and estimated as functions of reciprocal binary diffusivities. Second, the temperature, pressure, and composition dependence of binary diffusivities is unclear in a wide range of the thermodynamic scenario, and methods for correlation and/or prediction are continually being proposed. Among the haze of schemes, the methods based on an extended principle of corresponding states may be considered as the most attractive, their reliability depending on the initial theoretical assumptions and on the critical survey of the amount of available information.

Diffusion coefficients are generally very difficult to measure accurately. The rudimentary technique leads to scarce and divergent values. More sophisticated techniques, based on experiments carried out under severe boundary conditions, require an enormous volume of ancillary hardware. Furthermore, the apparatus are not commercialized and runs are very time consuming, not being feasible as laboratory routines.

In this work we shall present and discuss some diffusion data obtained by supercritical chromatography, a technique which, when operative, combines reliability and experimental simplicity.

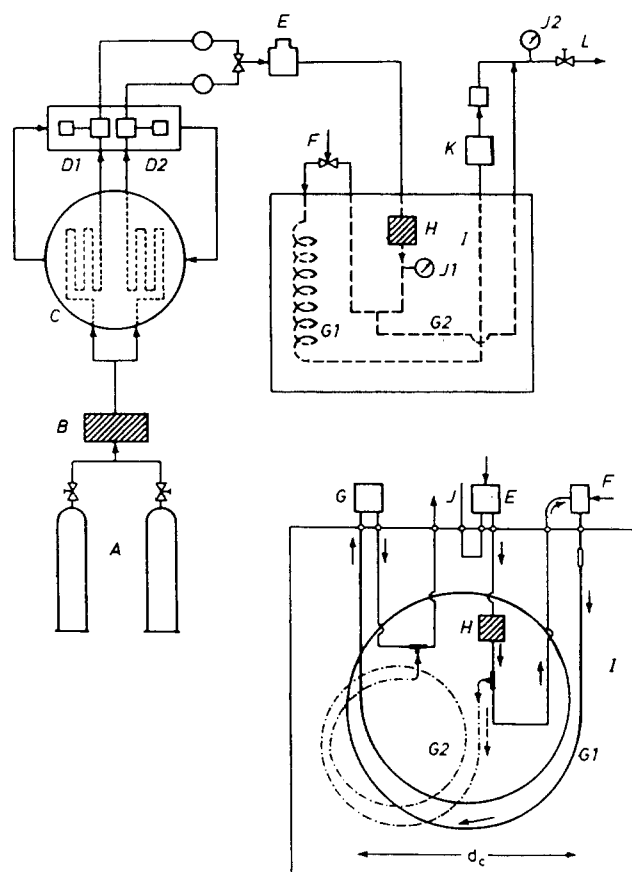


Figure 1. Flow diagram of the experimental device showing in more detail the improvements in the commercial configuration.

## Experimental Techniques

**a. Apparatus and Routine.** A modified HP-1082-B prototype of liquid chromatograph was used in our experiments. The basic commercial configuration (A, gas cylinders; B, mixer and primary filter; E, compressor; I, oven; J1,2, manometers), as Figure 1 shows, was complemented with the following items, in order to extend the range of effectiveness to the supercritical region: injection device and Rheodyne 7520 (F) valve with a 0.5- $\mu$ L loop, in order to operate with very small samples; UV-vis variable [190-600 nm] wavelength detector (K) thermostated and able to operate under extreme pressure conditions; double pump head (D) to achieve the uniform flow conditions required by the dispersion technique measurements; empty and large columns of stainless steel

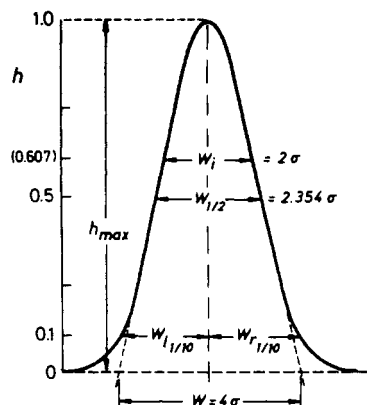


Figure 2. Parameters involved in the morphological description of a chromatographic peak.

tubing (G1) [30.48 m in length, 0.762-mm inside diameter], 26 cm being the coil diameter inside the oven; bypass and purge connected at the column inlet (G2) in order to achieve the low linear velocity required for diffusivity determination.

Constant flow rate and temperature ( $\pm 0.02$  cm<sup>3</sup>/min,  $\pm 0.1$  K) were maintained with a regulator operable from the console of the incorporated processor. Constant pressure ( $\pm 0.5$  bar) was assured by means of a manual pressure restrictor (TESCOM 1700) at the detector outlet (L). The pumps were refrigerated by means of an external exchanger (C) connected to a recirculating cold bath (HAAKE F-3-K) at  $-25$  °C by plastic jacketed tubing.

Samples of approximately  $0.5$   $\mu$ L were injected at room temperature into the slow laminar flow of the carrier, CO<sub>2</sub> (99.998% SEO), the retention time being about 2 h in all the experiments. A continuous operating mode has been followed, the samples being injected every 12 min up to the limit imposed by the software of the apparatus (327 min). Longer sets of experiments may be carried out with careful adjustments on the time reference for adequate plotting of the elution time. The chromatographic routine is followed in order to adjust the sensitivity and base line disturbances.

**b. Theoretical Background.** Grushka (1), Ouano (2), and Levenspiel (3) have demonstrated that, according to the statements of the work of Balenovic, Myers, and Giddings (4) and the Taylor (5–7) and Aris (8) dispersion techniques, the temporal variance of the Gaussian curve—which represents, at the time of elution, the concentration distribution of the initial narrow pulse of the solute that passes throughout the detector—may be interpreted as follows:

$$\sigma^2 = 2 \frac{D_e L}{\bar{u}_0} = \frac{2D_{12}L}{\bar{u}_0} + \frac{r_0^2 \bar{u}_0^2}{24D_{12}} \quad (1)$$

where  $D_{12}$  is the infinite dilution diffusivity of solute 1 in solvent 2,  $D_e$  is the apparent diffusivity or effective diffusion coefficient,  $L$  is the dispersion tube length,  $\bar{u}_0$  is the average velocity of the mobile phase,  $r_0$  is the dispersion tube inner radius, and  $\sigma^2$  is the variance of the curve in units of length

Figure 2 shows the nomenclature used to describe the chromatographic peaks,  $W_i$  being, according to Grushka (9) and Chesler (10), the parameter measured here for direct calculation of diffusivities.

According to the "height of the theoretical plate" ( $H$ ) or "relative peak broadening" concept, being

$$H = \sigma^2/L \quad (2)$$

eq 1 may be written as

$$D_{12} = (\bar{u}_0/4)\{H \pm [H^2 - (r_0^2/3)]^{1/2}\} \quad (3)$$

which provides values of  $D_{12}$  as a function of design parameters

( $r_0$  and  $L$ ) and experimental data ( $\bar{u}_0$  and  $\sigma^2$ ).

Both expressions allow the determination of the Marrero and Mason (11) effective diffusivity in the following way:

$$D_e = D_{12} + r_0^2 \bar{u}_0 / 48 D_{12} \quad (4)$$

The second term of the right-hand side of eqs 2 and 4 represents a deviation, thus evaluated by Levenspiel and Smith (3), of the dispersion (second temporal moment) of the average concentration curve predicted theoretically under severe boundary conditions, as a function of the axial distance  $x$  or time  $t$ .

### c. Procedure Criticism and Sources of Uncertainty.

**c.1. Flow Conditions and P-T Control.** According to Levenspiel and Smith (3), departure from the model is negligible in straight tubes when  $D_e/\bar{u}_0 L < 0.01$ . Giddings and Seager (12–14) have demonstrated that the significant root on eq 3 depends on the lineal velocity of the mobile phase, being used as the negative root when this value is over the optimal value ( $10^{-3}$  cm/s under supercritical conditions).

The tubing, injector, and detector are thermostated in order to avoid temperature gradients, being controlled by the software of the equipment. The pressure drop throughout the diffusion tube was less than 0.2 bar.

**c.2. Coiling Shape of the Column.** The use of large columns is one of the feasible procedures for obtaining adequate values of  $\sigma^2$ , and the only one available when the flux rate has operative limitations in its lower values. As a matter of fact, with the exception of craft prototypes, the commercial chromatographs are provided with small ovens, and the use of a coiling tube allows larger columns to be placed in reduced spaces.

The centrifugal forces which appear in the radial direction when the carrier fluid flows at high rates inside bending tubes determine a distortion on the solute plug. This effect has been previously treated in greater detail by other researchers such as Schneider (15), and must be identified by means of a thorough set of previous experiments in each column to be used, over a wide range of pressures and velocities of the mobile phase, in order to differentiate the narrowing of the solute plug from the influence of the flow rate in the position and dispersion on the eluted peaks.

The mathematical model may be applied to coiled columns with only a few restrictions in the hydrodynamics and mass transfer throughout the column, which may be summarized in the adimensional condition

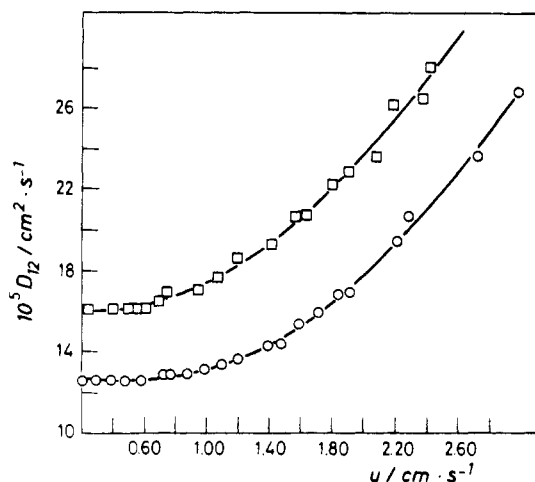
$$(De)(Sc)^{1/2} < 10 \quad (5)$$

in accordance with the Giddings (12–14), Koudski (16), Moulijn (17), Tjisen (18), Nunge (19), and Janssen (20) criteria.

**c.3. Injection of the Sample and Dead Volumes.** The real injection of the sample departs from the ideal inlet pulse due to the operative limitations of the ideal inflow and to the volume of the sample. Novotny and Springston (21) assume that an acceptable approach to the instantaneous injection may be obtained when injection times are less than 0.5 s, conditions very accessible for the modern injection valves.

The injection valve, detector, and connecting tubing may contribute to some extent to the total amount of dead volumes and so to the variance, according to the increase in the plate height predicted by Giddings (12–14). Widenings and contractions in the column-detector and column-injector fittings have been carefully avoided in the equipment described here, the total dead volume not exceeding  $0.02$  mm<sup>3</sup>.

The infinite dilution conditions may be assumed only when experiments carried out with small samples in columns of different length do not show contributions of the initial variance of the pulse using a subtraction procedure [Giddings



**Figure 3.** Variation of the apparent diffusivity of benzene as solute as a function of the velocity of the supercritical carbon dioxide as eluent:  $P = 160$  bar;  $\circ$ , 40 °C;  $\square$ , 60 °C.

and Sternberg (22)]. The injector intercalates the sample, avoiding these disturbances.

The adsorption of the solute by inner walls may determine an appreciable asymmetry of the peaks and discrepancies in the elution time of different solvents. In our case, the eluted peaks show a good symmetry, proven by numerical [Kirkland asymmetry factor,  $(W_2/W_1)_{1/10} < 1.05$ ] as well as by geometrical (folding over) procedures, discrepancies being below 1%, in accordance with the criterion of Sassiati (23).

### Results and Discussion

All the sources of errors previously mentioned and discussed in great detail by other researchers, such as Alizadeh and co-workers (24), have been considered. The dispersion modulus observed was  $D_e/\bar{u}_0L = 4 \times 10^{-8} \ll 0.001$  (error less than 0.5%). The transfer modulus  $(De)(Sc)^{1/2} = 0.5 < 10$ , being  $r_0/r_0 = 340 > 100$ , which indicates that the curvature effect can be overlooked according to Giddings (12–14).

#### a. Velocity Dependence of the Apparent Diffusivities.

Figure 3 shows binary diffusion coefficients,  $D_{12}$ , under infinite dilution conditions, benzene being solute 1 and supercritical

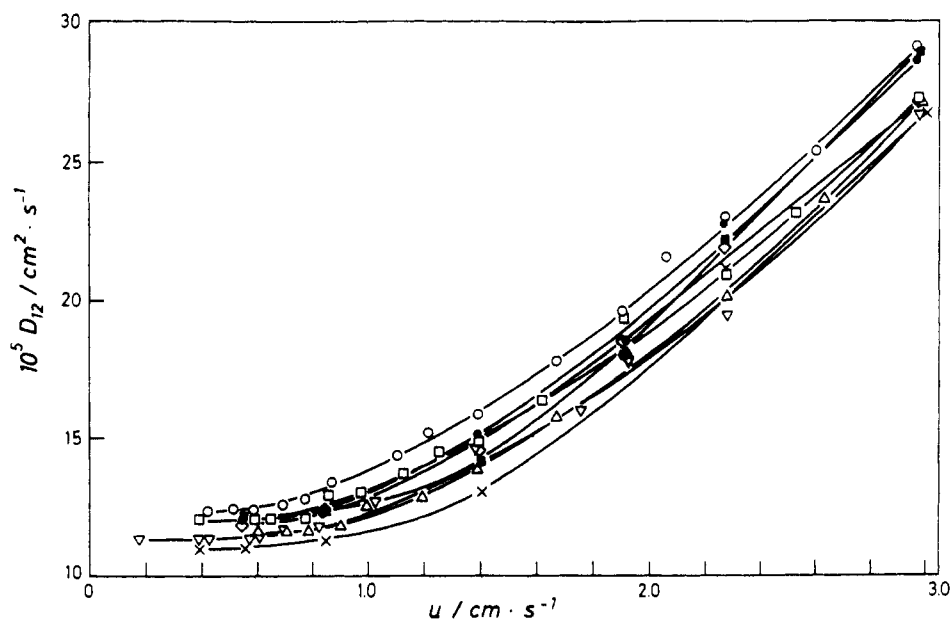
**Table I.** Diffusivity of Benzene in Supercritical Carbon Dioxide under Infinite Dilution Conditions as a Function of Pressure and Temperature

$T/^\circ\text{C}$	$10^5 D_{12}/(\text{cm}^2 \cdot \text{s}^{-1})$				
	$P = 150$ bar	$P = 200$ bar	$P = 250$ bar	$P = 300$ bar	$P = 350$ bar
40	12.99	11.20	10.27	9.67	9.01
50	15.58	12.97	11.72	11.10	10.58
60	18.18	15.40	13.60	12.44	11.57

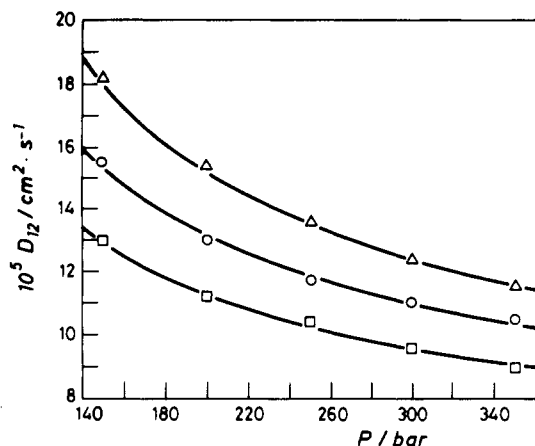
carbon dioxide being solvent 2, as a function of the average velocity of the carrier phase, at 40 and 60 °C and 160 bar, showing analogous morphology. Figure 4 shows the equivalent results obtained here for toluene, ethylbenzene, *n*-propylbenzene, cumene, *o*-xylene, *m*-xylene, *p*-xylene, and mesitylene at 40 °C and 160 bar in a coiled column 26 cm in diameter, 3048 cm in length, and 0.762 mm in inside diameter, illustrating the low flux region where the assumptions and prerequisites of the model are fulfilled and the diffusion coefficients tend toward their phenomenological constant values. These experiments demonstrate the regular tendency of all the compounds tested and so allow undertaking much work on the characterization of the optimal region for routine determinations that may be established below  $0.6 \text{ cm} \cdot \text{s}^{-1}$  to be avoided, in spite of higher values reported in recent papers [Olesik (25)].

**b. True Infinite Dilution Binary Diffusion Coefficients.** The optimal velocity of the carrier phase was reached and maintained in the range  $0.30\text{--}0.45 \text{ cm} \cdot \text{s}^{-1}$ . Each experiment was repeated six times to test the procedure, obtaining very good reproducibility. The results at 40 °C and 160 bar are shown in Table I, listed from higher to lower values of the diffusion coefficient.

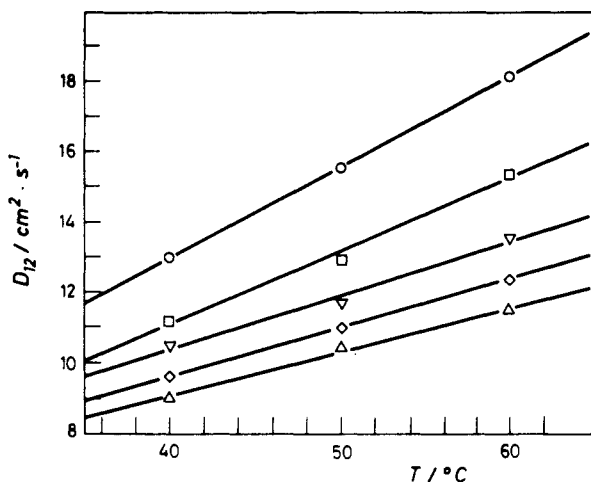
**c. Variability of Diffusion with State Properties.** As a first step in the search for a generalized correlation, the binary diffusion coefficient of benzene have been determined at several pressures and temperatures, the results being shown in Figures 5 and 6 (Table I), which respectively represent the variation of  $D_{12}$  as a function of pressure at constant temperature and  $D_{12}$  as a function of temperature at constant pressure. As shown in Figure 7, our data are in good agreement with those of Swaid and Schneider (26) and Lauer (27), all



**Figure 4.** Variation of the apparent diffusivity of several solutes as a function of the linear velocity of the supercritical carbon dioxide as solvent at 40 °C and 160 bar:  $\circ$ , toluene;  $\square$ , ethylbenzene;  $\bullet$ , *o*-xylene;  $\diamond$ , *m*-xylene;  $\blacksquare$ , *p*-xylene;  $\triangle$ , *n*-propylbenzene;  $\nabla$ , isopropylbenzene;  $\times$ , mesitylene.



**Figure 5.** Isothermal binary diffusion coefficients of benzene in carbon dioxide under infinite dilution conditions: □, 40 °C; ○, 50 °C; △, 60 °C.



**Figure 6.** Isobaric binary diffusion coefficients of benzene in carbon dioxide under infinite dilution conditions: ○, 150 bar; □, 200 bar; ▽, 250 bar; ◇, 300 bar; △, 350 bar.

of them systematically lower than the values published by Sassiat (23) at 40 °C. The data reported here extend the scenario previously described in the Introduction.

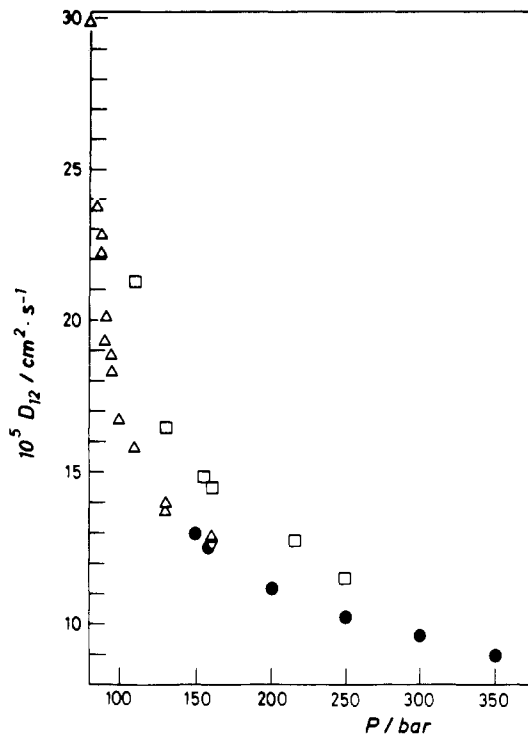
**d. Reduced Diffusivities.** The diffusivities of benzene have been correlated according to the extension of the Enskog theory, able to modelize binary diffusivities in the dense region. The Enskog-Thorne model correlates reduced diffusivities following the form

$$F \equiv D_{12}\rho / (D_{12}\rho)_0 \equiv D_r \quad (6)$$

in the coordinates referring to the low-density condition at the same temperature as an empirical function of a macroscopic property (density of the carrier) and molecular parameters (collision diameter and molecular mass)

$$D_r = \frac{1}{1 + 1.261\sigma_2^3 \left\{ \frac{\sigma_2 + 4\sigma_1}{4\sigma_2 + 4\sigma_1} \right\} \frac{\rho_2}{M_2}} \quad (7)$$

expressing  $\sigma$  in angstroms,  $M$  in grams per mole, and  $\rho$  in grams per cubic centimeter. The results presented in Table II have been obtained as follows: values of  $D_{r, \text{calcd}}$  were calculated from raw data given by Reid, Sherwood, and Prausnitz (28), and the density of  $\text{CO}_2$  was taken from ref 29; the value of  $(D_{12}\rho)_0$  for the reduction of experimental data was calculated from ref 26,  $\sigma_1$  from ref 30, and  $\sigma_2$  from ref 31.



**Figure 7.** Comparison between our data and those previously reported in the literature of benzene- $\text{CO}_2$  in the supercritical region: △, Swaid and Schneider, 1979; □, Sassiat et al., 1987; ▽, Lauer et al., 1983; ●, present work.

**Table II.** Enskog-Thorne Factor for Benzene in  $\text{CO}_2$ <sup>a</sup>

$T/^\circ\text{C}$	$P/\text{bar}$	$\rho/(\text{g}\cdot\text{cm}^{-3})$	$10^4 D_{12}/(\text{cm}^2\cdot\text{s}^{-1})$	$D_{r, \text{exptl}}$	$D_{r, \text{calcd}}$
40	150	0.7810	1.299	0.939	0.514
40	200	0.8408	1.120	0.871	0.496
40	250	0.8807	1.027	0.837	0.484
40	300	0.9112	0.967	0.815	0.456
40	350	0.9361	0.901	0.780	0.469
50	150	0.7008	1.558	1.010	0.541
50	200	0.7849	1.297	0.942	0.513
50	250	0.8350	1.172	0.905	0.497
50	300	0.8714	1.110	0.895	0.487
50	350	0.9003	1.058	0.881	0.479
60	150	0.6071	1.818	1.021	0.577
60	200	0.7246	1.540	1.032	0.533
60	250	0.7872	1.360	0.990	0.512
60	300	0.8305	1.244	0.956	0.499
60	350	0.8638	1.157	0.924	0.489


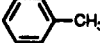

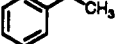
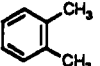
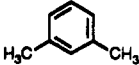
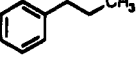
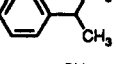
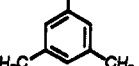
<sup>a</sup>  $(D_{12}\rho)_0 = 1.081$ ,  $\sigma_1 = 4.850$  Å, and  $\sigma_2 = 3.996$  Å.

## Conclusions

The work described here is part of a wider project concerning the generalized correlation of molecular diffusivities whose main objective and previous conclusion have been previously exposed in an introductory paper (32). It is well known that the correlation of binary diffusivities (e.g., in the form of state diagrams) involves greater difficulties than the adjustment of other transport properties, including autodiffusivities. With the exception of the ideal gas region, diffusivity varies with composition, it being necessary to introduce several definitions for the binary diffusion coefficient in a wide composition range (true diffusion, intradiffusion, tracer diffusion in a mixture) as well as in the limits when one solute tends to zero composition (infinite dilution diffusivities for each component). A review is carried out in ref 33.

The chromatographic technique is an experimental procedure able to provide diffusional data near the limit of trace concentration approaching zero, solving in part the uncer-

**Table III. Diffusivities of Benzene and Derivatives in Supercritical CO<sub>2</sub> at 40 °C and 160 bar**

compound		$10^6 D_{12}/(\text{cm}^2\text{s}^{-1})$
	benzene	12.60
	toluene	12.35
	<i>p</i> -xylene	12.16
	ethylbenzene	12.06
	<i>o</i> -xylene	12.06
	<i>m</i> -xylene	11.87
	<i>n</i> -propylbenzene	11.60
	cumene	11.36
	mesitylene	10.98

tainty derived from the true mean properties of the mixture. The systems tested here have been chosen for at least two reasons.

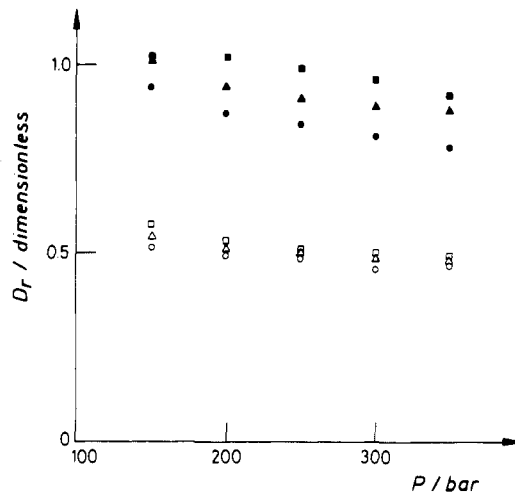
Binary diffusion in compressed gases is needed in modeling fluid extraction columns, an innovative and competitive procedure for the recovery of oligocompounds and valuable fractions of manufactured or natural products. The properties of carbon dioxide make it an excellent extractive reagent, and commercial equipment is able to handle supercritical CO<sub>2</sub> and aromatic compounds without problems.

From another point of view, the selected solutes and the experimental conditions at which the experiments were carried out are very useful in providing the data missing in the near critical region, dealing with the elucidation of group contributions of homologous series and with the extension of a generalized correlation for the prediction of gas diffusion coefficients based on the corresponding states principle.

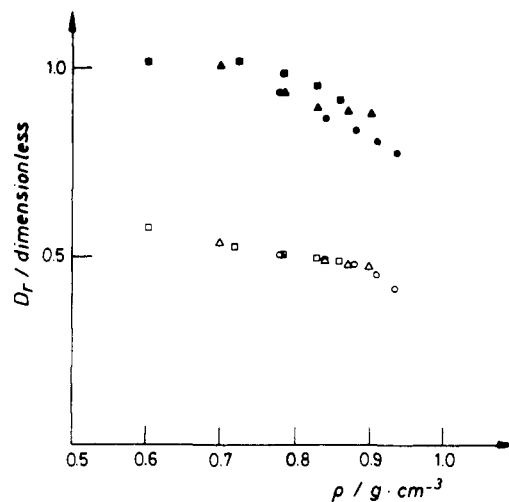
In fact, the experimental conditions described here represent, in the case of benzene, an extension of the region previously described in the literature, and preliminary conclusions can be outlined as follows.

Figure 4 is devoted to demonstrating that the dependence of the apparent diffusivity on the carrier velocity varies monotonously for all the systems when this condition departs from the model conditions. This is very important as it makes it necessary that all the equipment be calibrated carefully before initiating a systematic experimentation and suggests that these conditions (in our case linear velocity of the flow below 0.6 cm·s<sup>-1</sup>) may be considered independent of the nature of the solvent to be tested.

As was shown in Table III,  $D_{12}$  decreases when molecular weight and branching increases. Thus, benzene shows the highest value of diffusivity, a stretched molecule such as *p*-xylene diffuses faster than "ortho" and "meta" isomers, and *n*-propylbenzene diffuses better than its structural isomers cumene and mesitylene. The slight difference between the diffusivities of *o*-xylene and *m*-xylene and these with respect to *p*-xylene in all the region studied perhaps



**Figure 8.** Enskog-Thorne reduced diffusivity of benzene-CO<sub>2</sub> as a function of pressure:  $D_{r,\text{exptl}}$ , ●, 40 °C; ▲, 50 °C; ■, 60 °C;  $D_{r,\text{calcd}}$ , ○, 40 °C; △, 50 °C; □, 60 °C.



**Figure 9.** Enskog-Thorne reduced diffusivity of benzene-CO<sub>2</sub> as a function of density:  $D_{r,\text{exptl}}$ , ●, 40 °C; ▲, 50 °C; ■, 60 °C;  $D_{r,\text{calcd}}$ , ○, 40 °C; △, 50 °C; □, 60 °C.

needs an additional effort focused toward discussing whether there exists a preferential diffusion path in the direction of the axis of the molecule. It is hoped that it would be demonstrated in an extension of this work whether diffusivity ratios or departure between different compounds at different temperatures and pressures, within this series or within other series previously studied in the low density region (34), remain constant or vary significantly with temperature and pressure. We consider this way to be a suggestive approach in the line of group contribution formalism.

The variation of diffusivity with pressure and temperature observed with benzene-CO<sub>2</sub> agreed qualitatively but not quantitatively, for pressure rising from 150 to 350 bar at the three temperatures studied here, with respect to the data obtained below 150 bar. This requires more experimental effort in order to establish a numerical dependence  $D_{12}(P,T)$  in absolute or reduced coordinates.

In spite of the availability of more recent theories related to molecular dynamics, the Enskog-Thorne model is tested with our data in order to round off the conclusions of Swaid and Schneider (26) in the same line as Figures 8 and 9. As a matter of fact, the theoretical reduced diffusivities vary in the same manner as has been previously described, the experimental values being plotted above those calculated, as a proof of the failure of this theory explainable in terms of

a hydrodynamic description of the diffusion of molecules of different sizes and shapes. But our data in the same manner as theoretical values invert the rising tendency observed by Swaid and Schneider (26) below this pressure.

### Glossary

$D_{12}$	diffusivity of solute 1 in solvent 2
$D_e$	effective diffusion coefficient
$D_r$	reduced diffusivity
$d_c$	dispersion tube coiling diameter
$d_0$	dispersion tube inner diameter
$F$	Enskog-Thorne factor
$H$	height of the theoretical plate or relative peak broadening
$h$	height of the chromatographic peak
$L$	dispersion tube length
$M$	molecular weight
$P$	pressure
$r_c$	dispersion tube coiling radius
$r_0$	dispersion tube inner radius
$S_{10}$	Kirkland asymmetry factor ( $S_{10} = W_r/W_l$ )
$T$	temperature
$\bar{u}_0$	average linear velocity of the mobile phase
$W_l$	left semiwidth of the chromatographic peak (at $h/10$ )
$W_r$	right semiwidth of the chromatographic peak (at $h/10$ )
$De$	Dean number, $De = (\rho \bar{u}_0 / \eta)(d_c d_0)^{1/2}$
$Sc$	Schmidt number, $Sc = \eta / \rho D_{12}$
$\eta$	viscosity
$\sigma^2$	variance of the chromatographic peak
$\sigma_1$	collision diameter of the solute
$\sigma_2$	collision diameter of the solvent
$\rho$	density

### Subscripts

1	solute
2	solvent
12	tracer diffusion of 1 in 2

### Literature Cited

- (1) Grushka, E.; Maynard, V. *J. Chem. Educ.* 1972, 49, 565.
- (2) Ouano, A. C. *Ind. Eng. Chem. Fundam.* 1972, 11, 268.

- (3) Levenspiel, O.; Smith, W. K. *Chem. Eng. Sci.* 1957, 6, 227.
- (4) Balenovic, Z.; Myers, M. N.; Giddings, J. C. *J. Chem. Phys.* 1974, 78, 1564.
- (5) Taylor, G. *Proc. R. Soc. London* 1953, A219, 186.
- (6) Taylor, G. *Proc. R. Soc. London* 1954, A223, 446.
- (7) Taylor, G. *Proc. R. Soc. London* 1954, A225, 473.
- (8) Aris, R. *Proc. R. Soc. London* 1956, A235, 67.
- (9) Grushka, E.; Myers, M. N.; Schettler, P. D.; Giddings, J. C. *Anal. Chem.* 1969, 41, 889.
- (10) Chesler, S. N.; Cram, S. P. *Anal. Chem.* 1971, 43, 1922.
- (11) Marrero, T. R.; Mason, E. A. *J. Phys. Chem. Ref. Data* 1972, 1, 1.
- (12) Giddings, J. C.; Seager, S. L. *J. Chem. Phys.* 1960, 33, 1579.
- (13) Giddings, J. C.; Seager, S. L. *J. Chem. Phys.* 1961, 35, 2242.
- (14) Giddings, J. C.; Seager, S. L. *Ind. Eng. Chem. Fundam.* 1962, 1, 227.
- (15) Feist, R.; Schneider, G. M. *Sep. Sci. Technol.* 1982, 17, 261.
- (16) Koudsky, J. A.; Adler, R. J. *Can. J. Chem. Eng.* 1964, 42, 239.
- (17) Mouljijn, J. A.; Spijker, R.; Kolk, J. F. *J. Chromatogr.* 1977, 142, 155.
- (18) Tijssen, R. *Chromatographia* 1970, 3, 525.
- (19) Nunge, R. J.; Lin, R. S.; Gill, W. N. *J. Fluid Mech.* 1972, 51, 363.
- (20) Janssen, H. G.; Rijks, J. A.; Cramers, C. A. *J. High Resolut. Chromatogr.* 1990, 13, 474.
- (21) Novotny, M.; Springston, S. R. *J. Chromatogr.* 1963, 279, 417.
- (22) Sternberg, J. C. *Adv. Chromatogr.* 1966, 2, 205.
- (23) Sassi, P. R.; Mourier, P.; Caude, M. H.; Rosset, R. H. *Anal. Chem.* 1987, 59, 1164.
- (24) Alizadeh, A.; Nieto de Castro, C. A.; Wakeham, W. A. *Int. J. Thermophys.* 1980, 1, 243.
- (25) Olesik, S. V.; Woodruff, J. L. *Anal. Chem.* 1991, 63, 670.
- (26) Swaid, I.; Schneider, G. M. *Ber. Bunsen-Ges. Phys. Chem.* 1979, 83, 969.
- (27) Lauer, H. H.; McManigill, D.; Board, R. D. *Anal. Chem.* 1983, 55, 1370.
- (28) Reid, R. C.; Prausnitz, J. M.; Sherwood, T. K. *The Properties of Gases and Liquids*, 3rd ed.; McGraw Hill: New York, 1977.
- (29) *Liquid Chromatography Training Documentation*; Hewlett-Packard, 1980.
- (30) Sun, C. K. J.; Chen, S. H. *AIChE J.* 1985, 31, 1510.
- (31) Bird, R. B.; Stewart, W. E.; Lightfoot, E. N. *Fenómenos de Transporte (Transport Phenomena)*; Reverté: Barcelona, 1964.
- (32) Bueno, J. L.; Dizy, J.; Álvarez, R.; Coca, J. *Chem. Eng. Res. Des.* 1990, 68, 391.
- (33) Suárez, J. J.; Bueno, J. L.; Medina, I.; Dizy, J. *Afinidad* 1992, 438, 101.
- (34) Álvarez, R.; Medina, I.; Bueno, J. L.; Coca, J. *J. Chem. Eng. Data* 1983, 28, 155.

Received for review March 30, 1992. Revised July 28, 1992. Accepted January 27, 1993. The financial support of the CAICYT-2882/83 and CICYT ALL-90-0177 projects is gratefully acknowledged.